CKAP4 regulates the progression of vascular calcification in chronic kidney disease by modulating YAP phosphorylation and MMP2 expression

Yuping Shi
Shanghai Jiao Tong University School of Medicine
Xiucai Jin
Changhai Hospital
Man Yang
Shanghai Jiao Tong University School of Medicine
Jieshuang Jia
Shanghai Jiao Tong University School of Medicine
Hui Yao
Shanghai Jiao Tong University School of Medicine
Weijie Yuan
Shanghai Jiao Tong University School of Medicine
Kui Wang
Eastern Hepatobiliary Surgery Hospital
Shu Rong (sophiars@126.com)
Shanghai Jiao Tong University School of Medicine https://orcid.org/0000-0001-6140-2511

Research

Keywords: Vascular Calcification, VSMCs, CKAP4, YAP, MMP2, Chronic Kidney Disease

Posted Date: August 31st, 2020

DOI: https://doi.org/10.21203/rs.3.rs-60572/v1

Abstract

BACKGROUND

Vascular calcification (VC) is predominantly being associated with increased cardiovascular mortality and morbidity. In recent years, VC has been considered to be analogous to bone formation with parallels in biological processes such as osteogenic differentiation occurring in vascular smooth muscle cells (VSMCs). In this study, we aimed to understand the role of cytoskeleton-associated protein 4 (CKAP4), a type II transmembrane protein that is reversibly involved in the development of VC in chronic kidney disease (CKD).

METHODS

Mouse vascular smooth muscle cells (VSMCs) were isolated and treated with high phosphates (HP, 2.5 mmol/L Pi), and thus used as an in vitro model. And an in vivo mouse model of CKD induced by 5/6 nephrectomy and HP diet was developed.

RESULTS

Clinical analysis revealed that high levels of CKAP4 and MMP2 in serum were associated with CKD in patients. In both in vitro and in vivo models, we observed a significantly high expression of CKAP4, YAP and MMP2 both in VSMCs and calcified aorta. Alizarin red staining and calcium content assay reveled that silencing of CKAP4 reduced the VSMCs and aortic calcification, accompanied with reduced expression of YAP and MMP2. Additionally, by silencing CKAP4, we proved that CKAP4 is associated with nuclear translocation of YAP, which is an upstream regulator of MMP2.

CONCLUSIONS

We identified that CKAP4 could modulate yes-associated protein (YAP) phosphorylation and then alter gene expression of matrix metallopeptidase 2 (MMP2) during VC. These findings demonstrate for the first time that CKAP4 contributes to VC through modulation of YAP/MMP-2 pathway.

Introduction

Chronic kidney disease (CKD) is recently regarded as a major public health burden, given the growing incidence with a prevalence of 13% throughout the world[1, 2]. CKD could be categorized into five stages based on the renal glomerular filtration rates (GFR) with less than 60 mL/min per 1.73 m^2, considered as the moderate stage 3 CKD. Lower GFR levels leads to more severe progression of CKD, videlicet, severe stage 4 and end stage 5 CKD[3]. Subsequently, CKD progression is coupled with prevalence of other

complications such as vascular calcification (VC), cardiovascular disease (CVD), bone mineral disorder, hypertension and hyperlipidemia[4, 5]. Vascular function is usually characterized by three specific functions endothelial secretion, smooth muscle contraction, and integrity of the vascular structure. Abnormalities to one or all of these functions initiates at early stages of CKD simultaneously with cardiovascular issues and becomes more severe as end stage is reached [6]. CKD associated CVD projects in patients a risk for type 2 diabetes, and in these patients even with mild to moderate CKD the chance of atherosclerosis risk increase by 87% [7, 8]. Some patients experience a combinatorial severity of both renal bone disease and VC especially during hemodialysis, leading to difficulties with treatment options[9]. VC is considered as the mineral deposition in the vascular system, with calcification affecting intimal (atherosclerosis), medial layers (arteriosclerosis) of the arteries, or calcification in valves of the heart, thus contributing to the CVD risk factor[9].

Vascular smooth muscle cells (VSMCs) in the blood vessels play an important role by migrating to wounded areas in response to injury or stress, and restructure and repair these areas [10, 11]. Previously, studies have reported that calcification initiates in VSMCs through the release of vesicles containing hydroxyapatite [12]. Subsequently, this is proceeded by the active transformation of VSMCs towards an osteogenic or chondrogenic lineage, which further promotes the release of vesicular structures. The osteogenesis of these cells additionally promotes mineralization and release of multiple factors such as alkaline phosphatase (ALP) and bone morphogenic factor allowing complete transition of VSMCs towards osteogenic lineage [13]. On the other hand, in the vascular walls, the VSMCs passively recruits minerals from extracellular fluid and precipitates them, thus increased the mineralization[14]. VC is usually accompanied by elevated calcium and phosphate levels which in turn contributes to the vicious cycle of mineralization[13, 15]. Studies have shown that high-phosphate levels could contribute significantly to the CKD and is considered as a tool to develop models to understand disease progression[16, 17]. Interestingly, in a high phosphate environment, VSMCs seem to be unable to cope and undergo quick differentiation and apoptosis[15]. Even though, it is clear that VC is a vital contributor of complications and mortality in CKD patients, the molecular understanding behind VC development is not clear.

In this study, we aimed at understanding the molecular complications underlying the chronic kidney disease progression, to allow development of new diagnostic and therapeutic strategies.This study allows identification of the novel therapeutic targets and strategies to manage VC in CKD progression.

Materials And Methods

1. **Patients**

A total of 142 CKD patients including 57 men and 85 women aged from 40-76 were recruited from the Nephrology Department at Shanghai General Hospital between May 2018 and July 2019. In this study, 32 healthy patients with normal renal function were selected as the control group. All patients provided with

the signed consent forms. And, studies were performed in accordance with the declaration of Helsinki. The patient diagnoses are summarized in **Table 1**.

2. **VSMCs culture and treatments**

The VSMCs were isolated from the thoracic aorta of male Sprague-Dawley (SD) rats (n=5, 9-10 weeks) using the explants technique and cultured as previously described [16]. Briefly, cultured in M199 (Gibco, NY, USA) medium containing 10% fetal bovine serum (FBS) (Gibco) and 2 ng/ml basic FGF and were maintained at 37 °C in the presence of 5% CO_2. Complete medium replacement with fresh M199 medium was performed post 72 h. Within 2 weeks, cells emerged from the explant and confluency was achieved by 4 weeks. Smooth muscle identity was confirmed through α-smooth muscle actin (α-SMA) staining and the “hill and valley” growth patterning of the cells. Once the cells had undergone 5-8 passages, experiments were performed.

3. **Animal model**

Mice with a C57BL/6J background (Jackson Laboratory, Sacramento, CA) were used to develop the 5/6 Nx model. Further, the mice were kept at 12 h light and 12 h dark cycle in a (19–21°C) temperature-maintained facility with standard rodent diet and access to drinking water. The 5/6 Nx model (CKD model, *n* = 18 was developed on 16-week-old mice by decapsulating the left kidney through flank incision and resection of the upper and lower poles. Post 1 week, another surgery, specifically by incision in the right flank the right kidney was removed entirely. Sham group (*n* = 18) mice underwent similar surgical procedure except for the removal of right kidney. Post 1-week recovery, mice from both sham and CKD group were randomly split into groups with either a normal (0.5%) phosphate diet (*n* = 9) or high (1.5%) phosphate diet (*n* = 9) for 12 weeks. Further, after 12 weeks, using computerized tail-cuff system, blood pressure of the mice was measured. Urine was also assessed using ELISA kits (Assay Designs, Ann Arbor, MI) for creatinine and protein levels. Mice were anesthetized with isoflu-rane, exsanguinated successfully, renal and artery tissues were removed for further processing. These tissues were either quickly fixed and processed using Mason’s staining or flash frozen using liquid nitrogen and stored at -80 °C for further analysis.

4. **Calcium deposition**

To assess the deposited calcium, cells were initially decalcified for 24h using HCl (0.6 mol/L). Calcium concentration was measured by measuring the concentration of calcium in the HCL supernatant by atomic absorption spectroscopy and normalized to the protein content of cells measured using the BCA protein assay kit the BCA assay kit (Pierce, Rockford, IL) after solubilization in 0.1 M NaOH/ 0.1% sodium dodecyl sulfate.

5. **3-(4,5-Dimethylthiazol-2-yl)-2,5-diphenyltetrazolium bromide (MTT) assay**

To determine cell viability, VSMCs were seeded at a density of 4×10^3 cells/well on a 96 well plate. The cells were allowed to grow for 48 h and were incubated with MTT solution (Sigma Chemical Co., USA) at a concentration of 5 mg/ml at 37 °C. After 4 h of incubation, the MTT solution was removed and 100 µl DMSO was added. To allow complete solubility of the intracellular purple crystals, cells were incubated in an orbital shaker with DMSO for 5 mins. Further at 570 nm, absorbance was measured using a microplate reader (Thermo, Rockford, IL). Further, cell viability percentage was calculated using the formula “OD of treatment group/OD of control group * 100”.

6. **Alizarin red staining**

Calcification was determined using Alizarin red staining as previously described[18, 19]. Briefly, Alizarin S (100 mg) was dissolved in 10 mL of purified water and adjusted to pH 6.4 using a 0.1% KOH solution. Cells seeded onto 6 well plate were fixed using 70% ethanol and stained with Alizarin red. Further, the accumulated stain was dissolved using ethylpyridium chloride and thus obtained supernatant was measured at 550 nm using a microplate reader.

7. **Measurement of alkaline phosphatase (ALP) activity**

Cells cultured on a 24 well plate were detached after reaching confluency and sonicated in the presence of 600 ul distilled water. Using a modified Lowry method, ALP activity was measured. Briefly, assay mixtures containing 0.1 M 2-amino-2-methyl-1-propanol, 8 mM p-nitrophenyl phosphate disodium, and 1 mM $MgCl_2$, were added onto the cell homogenates. Post 4 mins incubation at 37 °C, 0.1 N NaOH was used to inhibit the reaction. Further at 405 nm, absorbance was read using a microplate reader. Measurements *p*-nitrophenol was used to prepare the standard curve. Further, normalization of the values was achieved using protein concentrations which were measured from the sonicated samples using BCA method[20].

8. **Apoptosis assay**

Apoptotic cell death was assessed by staining the cells with Annexin-V FITC and PI- staining. Based on the manufacturer’s protocols, both attached and free-floating cells were collected and stained with Annexin V-FITC antibody and PI. Further, these cells were quantified using flow cytometry[21].

9. **Cell line and viral transduction**

Overexpression of CKAP4 was performed using a lentivirus designed cDNA obtained from OriGene (Rockville, MD). 293A cells were used for production of CKAP4 containing lentivirus. To attain efficient transduction, a multiplicity of infection (MOI) of 100 was used.

10. **Small interfering RNA (siRNA) or small hairpin RNA (shRNA) transfection**

NC-siRNA and CKAP4-siRNA were synthesized chemically at Suzhou GenePharma Co. Ltd. (Suzhou, China). Mouse CKAP4 gene was constructed into pcDNA3.1+HA vector by Life Technologies (Invitrogen,

California, USA), and the empty vector served as the negative control. The cells were cultured to attain 70-80% confluency, after which cells were transfected either with, NC-siRNA or CKAP4-siRNA using Lipofectamine 2000 (Invitrogen, California, USA) based on the manufacturer's instructions.

11. **Immunocytochemical staining**

Firstly, cells were washed twice with PBS for 10 mins. Subsequently, they were fixed with 4% paraformaldehyde for 10 mins and permeabilized using 0.5% Triton-X in 0.1 M Tris-buffered saline (TBS; pH 7.6). Further, the cells were quickly washed with PBS. The cells were blocked 3% goat serum in TBS. Then, the cells were incubated with YAP (ab52771, Abcam) and MMP-2 (ab97779, Abcam) *primary antibody diluted in TBS with normal goat serum (10%) for 1 h. Subsequently, the cells were incubated with the Alexa Red conjugated anti-mouse IgG (Molecular Probes) secondary antibody in TBS for 1 h. Nuclear staining was performed using Hoechst 33258. Subsequent imaging of the cells was performed usingLaser Scanningconfocal fluorescence microscope (Olympus FV1000S).*

12. **Immunohistochemical analysis**

Paraffin embedded tissue sections (1-2 μM) were used to perform immunohistochemical analysis. The sections were mounted onto SUPERFROST slides and incubated at 37 °C overnight. De-waxing in xylene and ethanol was followed by antigen-retrieval by boiling in microwave oven three times for 5 mins (pH 6.0, 0.94 ml Antigen Unmasking Solution (Vector Laboratories, Burlingame, CA, USA)/100 ml distilled water). Further, the slides were immersed in 3% hydrogen peroxide solution for 20 mins. Blocking was performed with 10% goat serum in PBS for 30 mins. Slides were incubated with primary antibodies against CKAP4 (ab84712, Abcam) overnight at 4°C which was subsequently followed by incubation with secondary antibody conjugated with hydrogen peroxidase for 30 mins. Visualization was achieved with the aid of 3-Amino-9-Ethylcarbazole (AEC) substrate chromogen (ADI-950-200-0003, WAKO) and utilized based on the manufacturer's instructions. The sections were stained with hematoxylin and dehydrated through the treatment with gradient ethanol. Finally, the sections were mounted and visualized.

13. **Biochemical parameters**

Serum creatinine and urea, urinary calcium and phosphorus concentrations were determined using an automatic analyzer system (Ilab 1800, Lexington, MA, USA). Serum FGF-23 (Immunotopics, San Clemente, CA, USA) and DKK1 levels (Enzo Life Sciences, Farmingdale, NY, USA) were determined by using commercial ELISA kits according to the manufacturer's protocol.

14. **Western blot analysis**

Cells were cultured in 6 well dishes for 48 h and the protein was extracted RIPA buffer containing 0.1% SDS . The extracted protein was quantified using BCA assay kit. 20 μg of protein denatured using Lamelli buffer were loaded and migrated using a 10-15% SDS-PAGE gel, transferred onto a nitrocellulose membrane. Blocking of the membranes were performed using 5% skim milk in PBST (PBS with 0.1% Tween-20) for 1 h. Further, the membranes were incubated with the same blocking buffer containing

either of the primary antibodies; anti-CKAP4 (Abcam, ab84712, 1:1000), anti-YAP (Abcam, ab52771, 1:2000), anti-α-SMA (Abcam, ab32575, 1:1000), anti-RUNX2 (Abcam, ab236639, 1:1000), anti-Pit1 (Abcam, ab273048, 1:2000), anti-GAPDH (Abcam, ab9485, 1:2500), anti-MMP2 (Abcam, ab92536, 1:1000), and anti-SM22α (bioss, bs-2163R, 1:1000). The blots were incubated at 4°C overnight. Further, the blots were washed with PBST thrice and 5 mins each. The membranes were subsequently incubated with secondary antibody conjugated with horse-radish peroxidase for 1 h at RT. The membranes were visualized using chemiluminescent reagent in accordance with the manufacturer's instructions. The quantitative results of western blot analysis were determined in Image J software (U. S. National Institutes of Health, Bethesda, MD, USA).

15. **QRT-PCR**

The total RNA in samples were isolated using TRIZOL reagent (Invitrogen). After quantification, cDNA was synthesized using the First-strand cDNA synthesis kit (Invitrogen). A light cycler (Roche) and FastStart DNA Master Plus SYBR green I kit (Roche) was used to perform the quantitative PCR. Further, the expression was normalized with the values obtained from GAPDH. The primers used in the study are summarized in Table 2. PCR conditions used in this study is a as follows 95°C for 15 s, 57°C for 30 s, and 72°C for 1 min.

16. **Statistical analysis**

Data presented in this study are representative of three independent experiments. The results are expressed as mean ± SD. The significance of the values was assessed using one-way analysis of variance (ANOVA) followed by Student's T-test. All the statistical analysis in this study was carried out using SPSS 16.0 software. $P < 0.05$ was considered statistically significant.

Ethics Statement

The present study was approved by the local investigational review board and written informed consent was obtained from all participants.

Results

1. **Expression of CKAP4 and MMP2 in patients with CKD**

Initially, we investigated the levels of CKAP4 and MMP2 in the CKD patients. We identified that patients with stage V CKD, who are considered to have end stage renal disease, had the highest levels of both CKAP4 and MMP2 when compared with normal patients. Additionally, CKAP4 and MMP2 levels were significantly upregulated even in stage III-IV CKD patients, indicating their potential role in CKD (**Fig. 1A, B**)

2. **High phosphates treated VSMCs based CKD *in vitro* model**

To further understand the roles of CKAP4 in CKD, we initially developed an *in vitro* VSMC model from umbilical veins as described in the methods section. Further, to induce calcification, the cells were treated with high phosphates (HP, 2.5 mmol/L Pi). Consequently, with increasing time (days) in culture, we could observe increased calcification through alizarin red staining in the HP group when compared to both normal Pi (NP, 1.5 mmol/L Pi) and osmotic control (OC, NP+2.5 mmol/L D-mannitol) treatment groups (**Fig. 2A, B,** at day 7 $P < 0.01$). Alternatively, we also checked the ALP activity, which is an important indicator of CKD progression. It was evident that treatment with high phosphates (HP) could significantly increase the ALP levels (**Fig. 2C,** $P < 0.01$). These evidences supported our hypothesis that cells treated with high phosphates could be ideal *in vitro* models for CKD. Further, to understand the consequence of CKD progression on the expression profile of smooth muscle cell and osteogenic cell markers, the VSMCs were treated with differentiation medium for 2 weeks to direct them either towards smooth muscle cell or osteogenic lineage. Interestingly, we observed cells in HP treatment group expressed high levels of CKAP4, decreased α- smooth muscle actin (SMA; an adult smooth muscle marker [22]), and decreased smooth muscle protein α (SM22α, a maker for vascular smooth muscle[23]) indicating a limitation in differentiation towards the smooth muscle lineage. Alternatively, we observed an increased expression of pituitary-specific positive transcription factor (PIT-1, bone mineralization factor [24]), increased runt-related transcription factor 2 (Runx2, osteoblast differentiation factor [25]), and increased msh homeobox 2 (MSX2, bone development marker [26]). Above-mentioned results further affirmed that our cell model mimics the CKD progression through decreased smooth muscle differentiation and increased osteogenesis (**Fig. 2D, E**). Interestingly, we observed decreased cell viability in HP treated group using MTT assay (**Fig. 2 F,** $P < 0.01$). It was also evident from our Annexin-V flow cytometric analysis that HP treatment caused a severe 40% increase in apoptosis (**Fig. 2 G, H,** $P < 0.001$). This was further affirmed through the increased cleaved caspase-3 and Bax expression in the HP treatment group (**Fig. 2 I , J,** $P < 0.01$).

3. **Knockdown of CKAP4 reduces vascular calcification**

To further elucidate the molecular players in CKD, using siRNA technology we silenced CKAP4 in VSMCs and treated it with HP. Initially, we affirmed the successful silencing through decreased mRNA ($P < 0.001$, **Fig. 3A**) and protein levels in the si-CKAP4 (**Fig. 3B**). Evidently, sile ncing also decreased both calcification (**Fig. 3C**) and ALP activity levels (**Fig. 3D,** $P < 0.01$). This was supported by the fact, silencing of CKAP4 increased α-SMA, SM22α levels whereas it decreased PIT1, Runx2, MSX2 levels (**Fig. 3E**). This clearly indicated that lack of CKAP4 decreases osteogenesis and increased smooth muscle lineage. Additionally, we also observed increased cell viability (**Fig. 3F**) and decreased apoptosis (**Fig. 3G**, **H**; $P < 0.001$) in the absence of CKAP4. The decreased apoptosis was also confirmed through decreased cleaved caspase-3 and Bax levels (**Fig. 3I, J,** $P < 0.01$). Hence, the results indicate that CKAP4 could potentially play a vital role in the progression of CKD, through the regulation of VSMCs' differentiation towards osteogenic lineage rather than the smooth muscle lineage.

4. **CKAP4 is associated with nuclear translocation and phosphorylation of YAP**

We further wanted to elucidate the molecular consequences of CKAP4, and were interested in a MMP2 regulator, Yes-associated protein (YAP). We identified that lack of CKAP4 causes a translocation of YAP, which is usually localized in the nucleus. Immunofluorescence staining showed ~50% decrease in nuclear localization of YAP after silencing CKAP4 (**Fig. 4A,B,***P* < 0.01). Hence, it could be possible that in the absence of CKAP4 there was an increased p-YAP-ser 127 protein which is considered the cytoplasmic version of YAP protein. Antibody identifying the nuclear and full version of the YAP showed decreased levels in the siCKAP4 cells. Further, as YAP is a core component of the HIPPO pathway, we wanted to check the influence of CKAP4 on other HIPPO components such as large tumor suppressor 1/2 (LATS1/2) and mammalian sterile 20-like kinase 1/2 (MST1/2) and its phosphorylated versions. Evidentially, in the absence of CKAP4, LATS1/2 and MST1/2 were slightly decreased, when compared to the control group. However, the phosphorylated versions of both of these proteins where higher than the control group (**Fig. 4C**). This indeed mimicked the consequences observed in the YAP protein, indicating CKAP4 potentially affects CKD progression through the regulation of the HIPPO pathway.

5. **YAP is an upstream regulator of MMP2**

As previous studies have indicated YAP as an upstream regulator of MMP2[27], and in our study, we observed a high expression of MMP2 in the CKD patients, we wanted to check the effect of siYAP on MMP2 levels. Using immunofluorescence staining, we identified and confirmed that lack of YAP decreased MMP2 levels significantly (**Fig 5A**). Additionally, this was confirmed using western blot analysis of the protein (**Fig 5B**). Interestingly, silencing of YAP also caused a severe decrease in calcification, as observed through alizarin red staining (**Fig 5C**).

6. **CKAP4 promotes VSMCs calcification via YAP/MMP-2 pathway**

Further, we wanted to elaborate CKAP4s' activity in VSMC calcification. We studied the expression profile of smooth muscle and osteogenic markers in VSMCs with either siCKAP4, siCKAP4+OV-MMP2 (silence CKAP4 and overexpression of MMP2), OV-CKAP4 (overexpression of CKAP4), or OV-CKAP4+siMMP2 (overexpression of CKAP4 and silencing of MMP2). We subsequently performed qRT-PCR and western blotting analysis for all the markers. Initially, it was evident that when we overexpressed CKAP4; YAP, PIT1, Runx2, Msx2 were upregulated whereas α-SMA, SM22α were downregulated when compared with the silenced CKAP4 (**Fig. 6A-H**). In both siCKAP4+OV-MMP2 and OV-CKAP4+siMMP2 VSMCs, YAP, PIT1, Runx2, Msx2 were upregulated whereas α-SMA, SM22α were downregulated when compared with the silenced CKAP4. However, when compared with OV-CKAP4; YAP, PIT1, Runx2, Msx2 were decreased in siCKAP4+OV-MMP2 and OV-CKAP4+siMMP2 VSMCs (**Fig. 6A-H**). Additionally, when we compared siCKAP4+OV-MMP2 and OV-CKAP4+siMMP2 groups, even in the absence of MMP2 just CKAP4 overexpression could increase VSMC calcification. These evidences indicated that CKAP4 is sufficient to promote osteogenesis and calcification in VSMCs, and it regulated CKD progression through YAP/MMP2 pathway.

7. **High phosphate diet promotes CKAP4 expression *in vivo***

To further validate our observations, we developed an *in vivo* 5/6 nx mice model (CKD model), with high phosphate (Pi) diet. Serum and urinary parameters were shown in Table 3. The results showed that serum creatinine and urea levels in CKD group were higher than those in the control group. As expect, serum DKK1 and FGF-23 was significantly increased in both control and CKD mice supplemented with high Pi. Besides, we observed mice in the CKD model group, had a high CKAP4 and MMP2 levels compared to the sham group (**Fig. 7A-C**). However, high Pi diet in the CKD model group seems to further exacerbate the disease by a higher increase in CKAP4 and MMP2 levels when compared to normal Pi group (**Fig. 7A-C,** $P < 0.05$). These observations were confirmed using immunostaining of vascular tissue, which showed a severe CKAP4 increase in high Pi + CKD group (**Fig. 7D**), when compared with all the other groups.

8. **High phosphate induces aortic calcification in a high CKD model**

To further validate the *in vivo* model, we checked the calcification in the aorta using alizarin red staining. It was clear the CKD model with high Pi diet had increased calcification in aorta (**Fig. 8A**). Subsequently, we also confirmed the above-mentioned observations by quantifying the deposited calcium through absorption spectroscopic methods (**Fig. 8B,** $P < 0.05$ for sham normal Pi vs. high Pi; $P < 0.001$ for CKD normal Pi vs. high Pi). Further, we observed in high Pi diet- CKD model, osteogenic markers (*viz.*, PIT1, Runx2, Msx2) were highly upregulated. However, smooth muscle markers (viz., α-SMA, SM22α) were highly downregulated (**Fig. 8C**). ALP activity was significantly higher in the both normal and high Pi-CKD group, when compared with sham group (**Fig. 8D,** $P < 0.05$ for sham normal Pi vs. high Pi; $P < 0.05$ for CKD normal Pi vs. high Pi; $P < 0.01$ for sham normal Pi vs. CKD normal Pi). However, ALP activity was most significantly increased in the high Pi-CKD group. Similarly, apoptotic rate was most severe in the high Pi-CKD group (**Fig. 8E, F,** $P < 0.05$ for sham normal Pi vs. high Pi; $P < 0.01$ for CKD normal Pi vs. high Pi; $P < 0.001$ for sham normal Pi vs. CKD normal Pi). This was subsequently confirmed with cleaved caspase 3 and Bax levels being most high in high Pi-CKD group (**Fig. 8 G-I,** $P < 0.05$ for sham normal Pi vs. high Pi; $P < 0.05$ for CKD normal Pi vs. high Pi; $P < 0.05$ for sham normal Pi vs. CKD normal Pi). Even though, 5/6 nx CKD model could be the chief contributor for the CKD in these mice models, it was evident that its combination with high Pi diet leads to a severe CKD model.

9. **CKAP4 inhibition attenuates vascular calcification in CKD mice**

We additionally established another mice model, wherein CKD mice were administered with either vehicle or siCKAP4 (ad-CKAP4) lentivirus via tail vein injection and kept on high Pi diet for 12 weeks. Subsequently, the mice were sacrificed and tissues were assessed for calcification. It was clear that silencing of CKAP4 decreased calcification as observed through decreased alizarin red staining and aortic calcium levels (**Fig. 9A, B**). Additionally, western blotting data also indicated that in high Pi-CKD model with ad-CKAP4, there was significantly lower YAP and MMP2 levels (**Fig. 9C,** $P < 0.001$ high Pi+ad-CKAP4 *vs.*, Sham $P < 0.001$ high Pi+ad-CKAP4 *vs.*, high Pi +vehicle). These results indicated that CKAP4 inhibition attenuates VC through regulation of YAP and MMP2.

Discussion

CKAP4, a transmembrane protein, has been identified to be a cell surface receptor for many proteins such as tissue plasminogen activator (t-PA) and anti-proliferative factor (APF) [28, 29]. In cancer, CKAP4 by binding to APF, decreases the proliferation of bladder cancer cells [30, 31]. Interestingly, t-PA is upregulated in VSMC and human atherosclerotic disease, potentially as a response to vascular injury. Previous studies have indicated, t-PA binds to CKAP4 and acts as a plasminogen activator[32]. However, in our study, we identified CKAP4 to be highly upregulated in CKD patients (Fig. 1), CKD *in vitro* and *in vivo* models (Fig. 2, 7). Additionally, we observed in these models increased calcification, ALP activity, and apoptosis (Fig. 1, 2, 7). In the VSMC model, under a high phosphate environment, cells underwent osteogenic differentiation and highly expressed markers such as Runx2, Msx2, PIT1 but had decreased expression of α-SMA and SM22α (Fig. 2D). In VC, previous studies have identified that the osteogenesis is enhanced through the activation of Wnt signaling[26]. Additionally, it is elucidated that Wnt signaling causes osteogenic stimulation through activation of Runx2 expression[33]. Additionally, in the Wnt signaling pathway, prevention of proteasomal degradation of β-catenin, allows its activation and nuclear translocation. This activation of β-catenin, which is a transcriptional regulator of many downstream targets, allow the osteoblast to proliferate and mature[34]. However, the role of CKAP4 in enhancing osteogenesis, VC and CKD has been relatively unknown.

In the current study, we identified MMP2 to be highly expressed in patient's serum (Fig. 1B). Interestingly, silencing of CKAP4 decreased MMP2 expression, calcification, and osteogenic differentiation (Fig. 3). Previously, studies have clearly indicated that MMP2 could be the key factor involved in exacerbating the severity of CKD [6]. Additionally, it is well established that MMP2 is chiefly upregulated under oxidative stress and its expression has been known to decrease smooth muscle contraction[35–37]. In a study by Chung *et al.*, [38] it was observed that increased expression of MMP2 has been associated with decreased glomerular filtration rate and renal function. Hence, it was clear that MMP2 was correlated with poor prognosis in CKD patients. However, to understand MMP2's role in CKD, it is important to understand how CKAP4 regulates MMP2. To answer this question, we focused on a upstream regulator of MMP2, YAP. In our study, we observed lack of CKAP4 decreased the nuclear localization of YAP (Fig. 4A, B). Additionally, it was clear that CKAP4 absence increased phosphorylation of this protein at serine 127, thereby decreasing its localization in the nucleus (Fig. 4C). As YAP is an important regulator of many genes, studies have indicated that YAP translocation from nucleus to cytoplasm could decrease gene transcription of its downstream targets[39]. Additionally, we also observed other HIPPO pathway factors, such as Mst1/2, Lats1/2 in the absence of CKAP4 was also significantly decreased (Fig. 4C). But the phosphorylated versions were increased when compared with the control. HIPPO factors in their phosphorylated versions (active HIPPO pathway) are sequestered in the cytoplasm and are found to be transcriptionally inactive. However, inactivation of the HIPPO pathway seems to correspond to nuclear translocation of the factors and activation of YAP[40, 41].

Interestingly, studies have also indicated YAP antagonists have protective and regenerative abilities in cancer and ischemia[22, 42]. In the study by Xu *et al.*, it was clearly indicated that constant increase in YAP

activation could cause interstitial fibrosis and abnormal differentiation of renal tubules [22]. However, in our study it was clear that nuclear localization and decreased phosphorylation of YAP, increased MMP2 activity and also aided in VC. Previously, many studies have indicated YAP as an upstream regulator of MMP2, in studies on gastric adenocarcinoma, knockdown of YAP significantly decreased MMP2 expression[43, 44]. Even in our study, we observed silencing of YAP significantly decreased MMP2 levels in the *in vitro* model (Fig. 5). We also successfully developed an 5/6 nx mice model with high phosphate diet, which showed increased calcification, ALP activity and higher osteogenic expression profile (Fig. 7). However, silencing of CKAP4 in the CKD mice model, showed significant decrease YAP, MMP2 and calcification (Fig. 8). This confirmed our hypothesis, CKAP4 modulates VC in CKD through modulation of YAP/MMP2 pathway.

Declarations

Availability of data and materials

The data during the current study are available from the corresponding author on reasonable request.

Acknowledgements

Not applicable.

Funding

The National Natural Science Foundation of China (No. 81970636).

Contributions

Yuping Shi and Xiucai Jin performed the experiments and drafted the manuscript; Mam Yang, Jieshuang Jia, Hui Yao and Weijie helped analyze the experimental data; YuanKui Wang conceived the idea, designed the experiments; Shu Rong designed the experiments, amend the manuscript. The authors declare no conflict of interest. All authors read and approved the final manuscript.

Ethics approval and consent to participate

All procedures were performed with respect to the guidelines and was approved by the Institutional Animal Care and Ethics committee at Shanghai Jiaotong university.

Competing interest

No potential conflicts of interest are disclosed.

Consent for publication

Not applicable.

References

1. Hill NR, FS T, OJ L, HJ A, OCC A, LD S, Richard HFD. & Giuseppe R. Global Prevalence of Chronic Kidney Disease – A Systematic Review and Meta-Analysis. *PLoS ONE* 11 e0158765-.
2. Brück K, Stel VS, Gambaro G, Hallan S, Völzke H, Ärnlöv J, Kastarinen M, Guessous I, Vinhas J, Stengel B, Brenner H, Chudek J, Romundstad S, Tomson C, Gonzalez AO, Bello AK, Ferrieres J, Palmieri L, Browne G, Capuano V, Van Biesen W, Zoccali C, Gansevoort R, Navis G, Rothenbacher D, Ferraro PM, Nitsch D, Wanner C. & Jager KJ. CKD Prevalence Varies across the European General Population. J Am Soc Nephrol. 2016;27:2135–47.
3. Paniagua-Sierra JR, Galván-Plata ME. Chronic kidney disease. *Revista medica del Instituto Mexicano del Seguro Social* 2017 **55** S116-S117.
4. Goldsmith D, Ritz E, Covic A. Vascular calcification: a stiff challenge for the nephrologist: does preventing bone disease cause arterial disease? Kidney Int. 2004;66:1315–33.
5. London GM, Marchais SJ, Guérin AP, Boutouyrie P, Métivier F, de Vernejoul M-C. Association of bone activity, calcium load, aortic stiffness, and calcifications in ESRD. J Am Soc Nephrol. 2008;19:1827–35.
6. Chung AWY, Yang HHC, Kim JM, Sigrist MK, Chum E, Gourlay WA, Levin A. Upregulation of matrix metalloproteinase-2 in the arterial vasculature contributes to stiffening and vasomotor dysfunction in patients with chronic kidney disease. Circulation. 2009;120:792–801.
7. Tuttle KR, Bakris GL, Bilous RW, Chiang JL, de Boer IH, Goldstein-Fuchs J, Hirsch IB, Kalantar-Zadeh K, Narva AS, Navaneethan SD, Neumiller JJ, Patel UD, Ratner RE, Whaley-Connell AT, Molitch ME. Diabetic kidney disease: a report from an ADA Consensus Conference. *Am. J. Kidney Dis.* 2014 **64** 510–533.
8. Papademetriou V, Lovato L, Doumas M, Nylen E, Mottl A, Cohen RM, Applegate WB, Puntakee Z, Yale JF, Cushman WC. Chronic kidney disease and intensive glycemic control increase cardiovascular risk in patients with type 2 diabetes. Kidney Int. 2015;87:649–59.
9. Wu M, Rementer C, Giachelli CM. Vascular calcification: an update on mechanisms and challenges in treatment. Calcif Tissue Int. 2013;93:365–73.
10. Kenagy RD, Vergel S, Mattsson E, Bendeck M, Reidy MA, Clowes AW. The role of plasminogen, plasminogen activators, and matrix metalloproteinases in primate arterial smooth muscle cell migration. 1996 16 1373.
11. Munro JM, Cotran RS. The pathogenesis of atherosclerosis: atherogenesis and inflammation. 1989 58 249–261.
12. Mathew S, Tustison KS, Sugatani T, Chaudhary LR, Rifas L, Hruska KA. The Mechanism of Phosphorus as a Cardiovascular Risk Factor in CKD. 2008 19 1092–1105.
13. Reynolds. & L. J. Human Vascular Smooth Muscle Cells Undergo Vesicle-Mediated Calcification in Response to Changes in Extracellular Calcium and Phosphate Concentrations: A Potential

Mechanism for Accelerated Vascular Calcification in ESRD. *Journal of the American Society of Nephrology* 15 2857–2867.

14. Cannata-Andia JB, Roman-Garcia P, Hruska K. The connections between vascular calcification and bone health. Nephrol Dial Transplant. 2011;26:3429–36.
15. Shroff RC, McNair R, Skepper JN, Figg N, Schurgers LJ, Deanfield J, Rees L, Shanahan CM. Chronic mineral dysregulation promotes vascular smooth muscle cell adaptation and extracellular matrix calcification. J Am Soc Nephrol. 2010;21:103–12.
16. Patel JJ, Bourne LE, Davies BK, Arnett TR, MacRae VE, Wheeler-Jones CP, Orriss IR. Differing calcification processes in cultured vascular smooth muscle cells and osteoblasts. Exp Cell Res. 2019;380:100–13.
17. Ge D, Meng N, Su L, Zhang Y, Zhang S-l, Miao J-y, Zhao J. Human vascular endothelial cells reduce sphingosylphosphorylcholine-induced smooth muscle cell contraction in co-culture system through integrin β4 and Fyn. Acta pharmacologica Sinica. 2012;33:57–65.
18. Kanazawa I, Yamaguchi T, Yano S, Yamauchi M, Yamamoto M, Sugimoto T. Adiponectin and AMP kinase activator stimulate proliferation, differentiation, and mineralization of osteoblastic MC3T3-E1 cells. *BMC Cell Biol.* 2007 8.
19. Lin X, Zhan J-K, Zhong J-Y, Wang Y-J, Wang Y, Li S, He J-Y, Tan P, Chen Y-Y, Liu X-B, Cui X-J, Liu Y-S. lncRNA-ES3/miR-34c-5p/BMF axis is involved in regulating high-glucose-induced calcification/senescence of VSMCs. Aging. 2019;11:523–35.
20. Li C, Chang Y, Li Y, Chen S, Chen Y, Ye N, Dai D, Sun Y. Advanced glycation end products promote the proliferation and migration of primary rat vascular smooth muscle cells via the upregulation of BAG3. *Int. J. Mol. Med.*.
21. Wu N, Lin X, Zhao X, Zheng L, Xiao L, Liu J, Ge L, Cao S. MiR-125b acts as an oncogene in glioblastoma cells and inhibits cell apoptosis through p53 and p38MAPK-independent pathways. *British Journal of Cancer* 109 2853–2863.
22. Xu J, Li P-X, Wu J, Gao Y-J, Yin M-X, Lin Y, Yang M, Chen D-P, Sun H-P, Liu Z-B. Involvement of the Hippo pathway in regeneration and fibrogenesis after ischaemic acute kidney injury: YAP is the key effector. *Clinical Science* 2016.
23. Raja. Chakraborty, Fatima, Zahra, Saddouk, Ana, Catarina, Carrao & Diane. Promoters to Study Vascular Smooth Muscle.
24. Lim K, Lu T-S, Molostvov G, Lee C, Lam FT, Zehnder D, Hsiao L-L. Vascular Klotho Deficiency Potentiates the Development of Human Artery Calcification and Mediates Resistance to Fibroblast Growth Factor 23. *Circulation* 125 2243–2255.
25. Steitz SA, Speer MY, Curinga G, Yang HY, Haynes P, Aebersold R, Schinke T, Karsenty G, Giachelli CM. Smooth muscle cell phenotypic transition associated with calcification: upregulation of Cbfa1 and downregulation of smooth muscle lineage markers. Circulation research. 2001;89:1147–54.
26. Martínez-Moreno JM, Muñoz-Castañeda JR, Herencia C, Oca AMD, Estepa JC, Canalejo R, Rodríguez-Ortiz ME, Perez-Martinez P, Aguilera-Tejero E. & Canalejo A. In vascular smooth muscle cells

paricalcitol prevents phosphate-induced Wnt/β-catenin activation. 2012 303 F1136.

27. Taha A. Mina, Ghahremani, Xiaolong & Yang. The Role of YAP and TAZ in Angiogenesis and Vascular Mimicry.
28. Conrads TP, Tocci GM, Hood BL, Zhang C-O, Guo L, Koch KR, Michejda CJ, Veenstra TD. & Keay SK. CKAP4/p63 Is a Receptor for the Frizzled-8 Protein-related Antiproliferative Factor from Interstitial Cystitis Patients. *Journal of Biological Chemistry* 281 37836–37843.
29. Bates SR, Kazi AS, Tao J-Q, Yu KJ, Gonder DS, Feinstein SI, Fisher AB. Role of P63 (CKAP4) in binding of surfactant protein-A to type II pneumocytes. *AJP: Lung Cellular and Molecular Physiology* 295 L658-L669.
30. Li SX, Liu L-j, Dong L-w, Shi H-g, Pan Y-f, Tan Y-x, Zhang J, Zhang B. Ding Z-w & Jiang T-y. CKAP4 inhibited growth and metastasis of hepatocellular carcinoma through regulating EGFR signaling. *Tumour Biol* 35 7999–8005.
31. Shahjee HM, Koch KR, Guo… L. Antiproliferative factor decreases Akt phosphorylation and alters gene expression via CKAP4 in T24 bladder carcinoma cells. 29 160.
32. Razzaq TM, Bass R, Vines DJ, Werner F, Whawell SA, Ellis V. Functional Regulation of Tissue Plasminogen Activator on the Surface of Vascular Smooth Muscle Cells by the Type-II Transmembrane Protein p63 (CKAP4). *Journal of Biological Chemistry* 278 42679–42685.
33. Gaur T, Lengner CJ, Hovhannisyan H, Bhat RA, Lian JB. Canonical WNT Signaling Promotes Osteogenesis by Directly Stimulating Runx2 Gene Expression. J Biol Chem. 2005;280:33132–40.
34. Nusse R, Clevers H. Wnt/β-Catenin Signaling, Disease, and Emerging Therapeutic Modalities. *Cell* 2017 169 985–999.
35. Wang W, Viappiani S, Sawicka J, Schulz R. Inhibition of endogenous nitric oxide in the heart enhances matrix metalloproteinase-2 release. Br J Pharmacol. 2005;145:43–9.
36. Chew DKW, Conte MS, Khalil RA. Matrix metalloproteinase-specific inhibition of Ca2 + entry mechanisms of vascular contraction. J Vasc Surg. 2004;40:1001–10.
37. Galis ZS, Khatri JJ. Matrix metalloproteinases in vascular remodeling and atherogenesis: the good, the bad, and the ugly. Circulation research. 2002;90:251–62.
38. Chung AW, Booth AD, Rose C, Thompson CR, Levin A, van Breemen C. Increased Matrix Metalloproteinase 2 Activity in the Human Internal Mammary Artery Is Associated with Ageing, Hypertension, Diabetes and Kidney Dysfunction. *Journal of Vascular Research* 45 357–362.
39. Sudol M, Shields DC, Farooq A. Structures of YAP protein domains reveal promising targets for development of new cancer drugs. *Seminars in Cell & Developmental Biology* 23 827–833.
40. Zhao B, Wei X, Li W, Udan RS, Yang Q, Kim J, Xie J, Ikenoue T, Yu J, Li L. Inactivation of YAP oncoprotein by the Hippo pathway is involved in cell contact inhibition and tissue growth control. *Genes & Development* 21 2747–2761.
41. Zhao B, Tumaneng K, Guan K-L. The Hippo pathway in organ size control, tissue regeneration and stem cell self-renewal. *Nat. Cell Biol.* 13 877–883.

42. Jiao S, Wang H, Shi Z, Dong A, Zhou Z. A Peptide Mimicking VGLL4 Function Acts as a YAP Antagonist Therapy against Gastric Cancer. Cancer Cell. 2014;25:166–80.
43. Zhang J, Xu ZP, Yang YC, Zhu JS, Zhou Z, Chen WX. Expression of Yes-associated protein in gastric adenocarcinoma and inhibitory effects of its knockdown on gastric cancer cell proliferation and metastasis. 2012 25 583.
44. Pan Z, Tian Y, Zhang B, Zhang X, Shi H, Liang Z, Wu P, Li R, You B. & Yang L. YAP signaling in gastric cancer-derived mesenchymal stem cells is critical for its promoting role in cancer progression. *International Journal of Oncology*.

Tables

Table 1. Clinical characteristics of healthy volunteers and patients with CKD.

	Healthy controls	CKD stage III-IV	CKD stage V
No. of cases	32	47	95
Age(years)	46.5 ± 6.5	57.9 ± 8.9*	60.2 ± 10.1**
Male gender(%)	56.2%	57.5%	61.1%
Hypertension(%)	—	55.2%	57.6%
Diabetes mellitus(%)	—	58.5%	67.2%
Serum creatinine(mg/dL)	0.63 ± 0.3	1.82 ± 0.25**	5.95 ± 0.37**
eGFR(mL/min/1.73m^2)	88.92 ± 4.4	29.85 ± 3.6**	13.8 ± 2.4**

Data are shown as mean ± SD. *p<0.05, **p<0.01.

Table 2. The sequence of primers used in the study.

Gene symbol	Sequence 5’—3’	Size(bp)
CKAP4-F	TCCCGTCAGAGGGATGAGC	106
CKAP4-R	GCTGGGAGTTTCTCAGGAGG	
MMP2-F	ACCTGAACACTTTCTATGGCTG	140
MMP2-R	CTTCCGCATGGTCTCGATG	
GAPDH-F	AGGTCGGTGTGAACGGATTTG	123
GAPDH-R	TGTAGACCATGTAGTTGAGGTCA	
YAP-F	TTGCGTCTGATCTCGTGGAG	137
YAP-R	GGAAGCTGTCTCATGCCTCA	
α-SMA-F	TCCACCGCAAATGCTTCTAAGT	121
α-SMA-R	ATGAGTCAGAGCTTTGGATAGGC	
SM22α-F	TGGTGAGCCAAGCAGACTTC	132
SM22α-R	AAGGCTTGGTCGTTTGTGGA	
Pit1-F	CAATTCCGCCTCTGCACCTA	117
Pit1-R	TTCACATGTGTGCTGGCTTC	
Runx2-F	CCGCCTCAGTGATTTAGGGC	131
Runx2-R	GGGTCTGTAATCTGACTCTGTCC	
MSX-F	GGAGCACCGTGGATACAGG	132
MSX-R	TAGAAGCTGGGATGTGGTGAA	

Table 3. Biochemical parameters between groups.

	Sham+Normal Pi (n=9)	Sham+High Pi (n=9)	CKD+Normal Pi (n=9)	CKD+High Pi (n=9)
Serum DKK1 (pg/mL)	387 ± 121	411 ± 132	612 ± 78[a]	1087 ± 139[a,b]
Serum FGF-23 (pg/mL)	421 ± 102	952 ± 69	681 ± 78[a]	21036 ± 2106[a,b]
Serum urea (mmol/L)	6.5 ± 0.4	6.9 ± 0.6	12.9 ± 0.8[a]	13.3 ± 1.1[a]
Serum creatinine (μmol/L)	17.2 ± 1.6	20.5 ± 0.7	43.6 ± 3.1[a]	65.7 ± 2.4[a,b]
Urinary calcium (mg/d)	0.035 ± 0.006	0.169 ± 0.053	0.084 ± 0.007[a]	0.126 ± 0.029[a,b]
Urinary phosphate (mg/d)	0.980 ± 0.091	4.126 ± 0.198	0.793 ± 0.057[a]	2.563 ± 0.231[a,b]

Values are expressed as mean ± SD. FGF-23, fbroblast growth factor-23; [a]p < 0.05 vs Sham; [b]p <0.05 vs Normal Pi

Figures

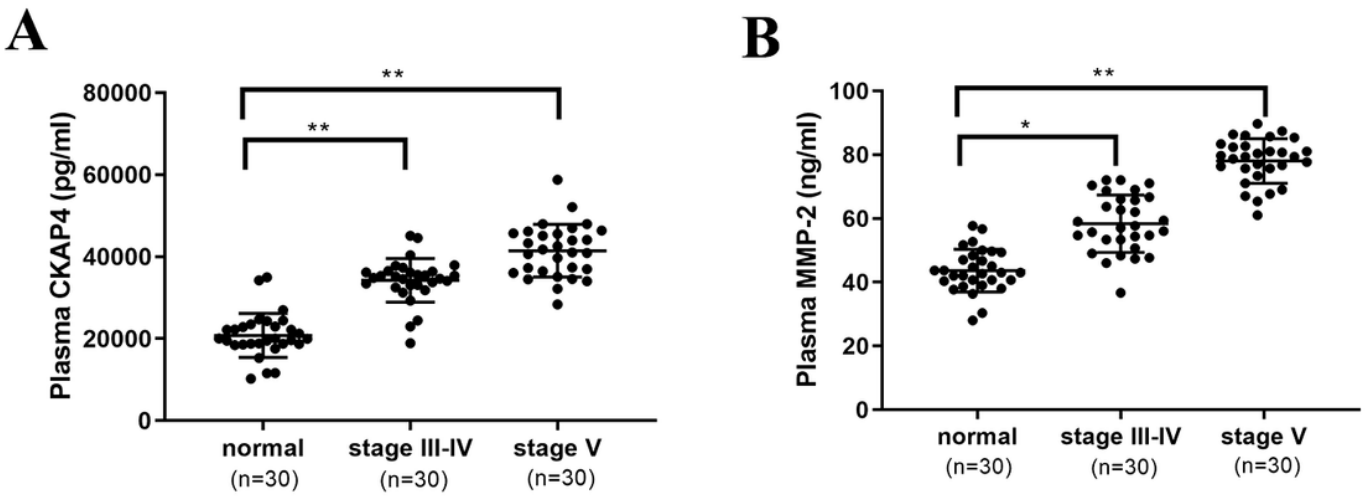

Figure 1

CKAP4 and MMP2 expression in the serum of patients with CKD. (A) CKAP4 levels and (B) MMP2 levels were detected using the ELISA kit, in patients' serum. The data are presented as mean ± SD **P < 0.01.

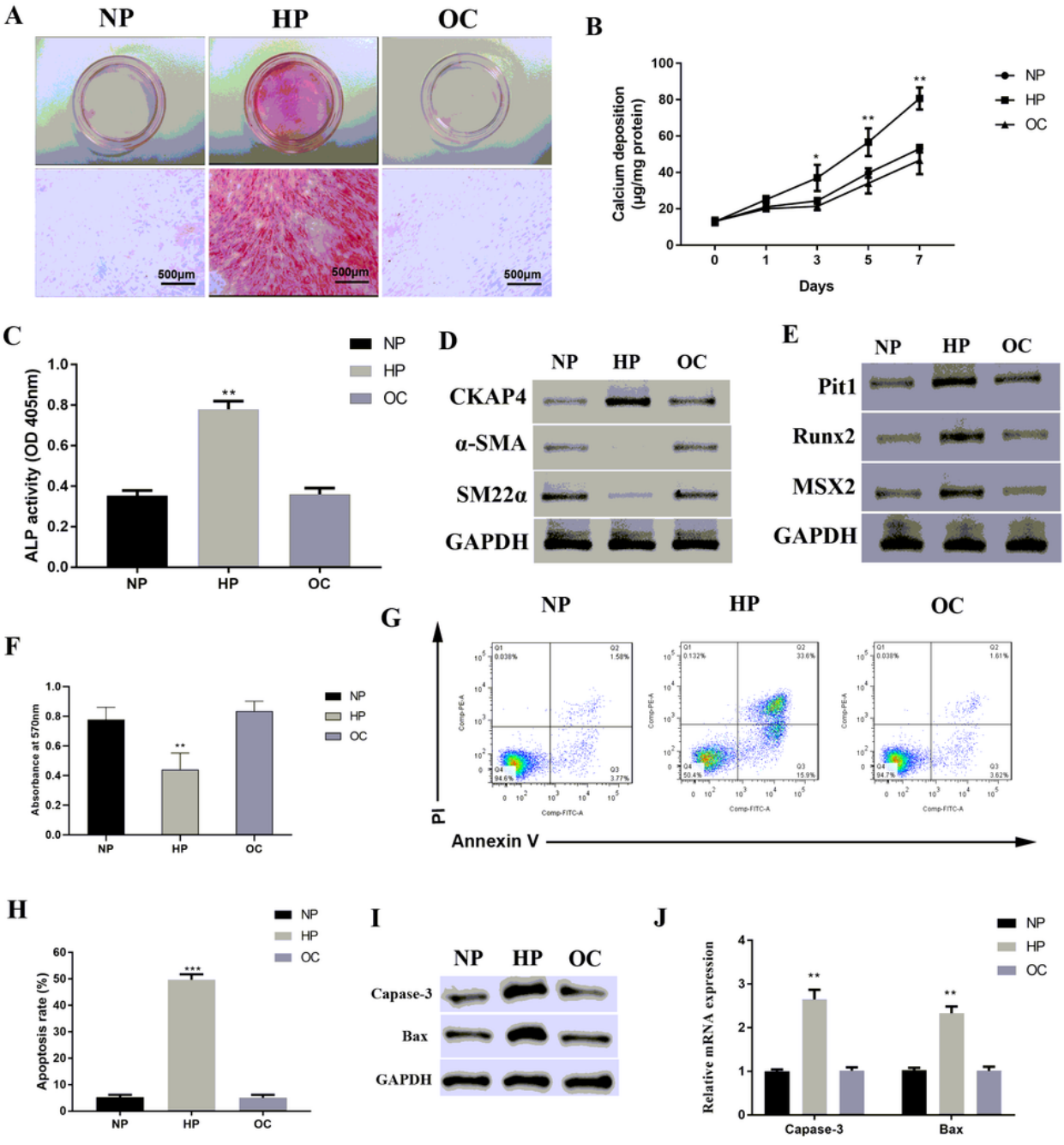

Figure 2

Treatment with high phosphates induces VSMCs calcification. (A) Alizarin red staining was performed on VSMCs incubated under different conditions for 14 days with a media replacement every 3 days. (B) Calcium content and (C) ALP activity was expressed as the mean ± SD of at least three simultaneous replicates. (D-E) Expression of CKAP4, smooth cell and osteogenesis markers were determined through western blotting in VSMCs exposed to differentiation medium for 2 weeks. (F) Cell viability was detected

using MTT assay. (G-H) Analysis of apoptosis rates were done using flow cytometry and quantification. Data are expressed as the mean ± S.E.M (n = 3). (I-J) Western-blot analysis of apoptosis related proteins (cleaved caspase 3 and Bax). NP: Normal Pi (1.5 mmol/L Pi), HP: High Pi (2.5 mmol/L Pi), OC：Osmotic control (NP+2.5 mmol/L D-mannitol). *P < 0.05,**P < 0.01 compared to the NP treatment group.

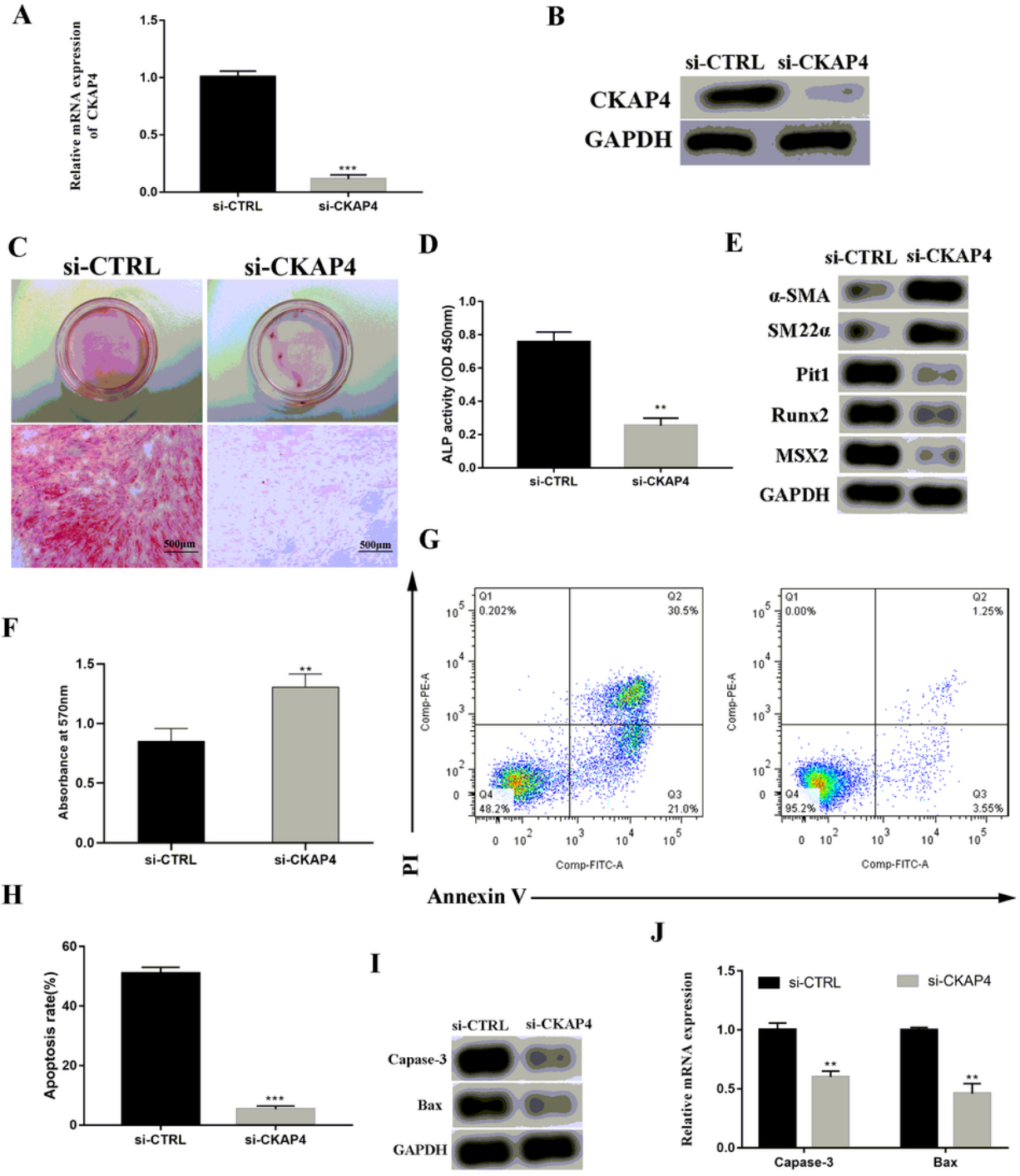

Figure 3

Knockdown of CKAP4 reduces vascular calcification. VSMCs were treated with negative control siRNA, or CKAP4 siRNA (siCKAP4) for 24 h, respectively. The mRNA (A) and protein (B) expression of CKAP4 in VSMCS detected by RT-PCR and western blot analysis, respectively. Cells were transfected with negative control siRNA, or CKAP4 siRNA for 24 h, respectively. (C) Alizarin red staining was performed on VSMCs incubated under different conditions for 14 days with changing media every 3 days. (D) ALP activity was expressed as the mean ± SD of at least three simultaneous replicates. (E) Expression of smooth cell and osteogenesis markers were determined by WB in VSMCs exposed to differentiation medium for 2 weeks. (F) Cell viability was detected using MTT assay. (G-H) Analysis of apoptosis rates by flow cytometry and quantification. Data are expressed as the mean ± SD (n = 3). (I-J) Western blotting analysis of apoptosis related proteins (cleaved caspase 3 and Bax). *P < 0.05,**P < 0.01, ***P < 0.001 compared to the si-CTRL group.

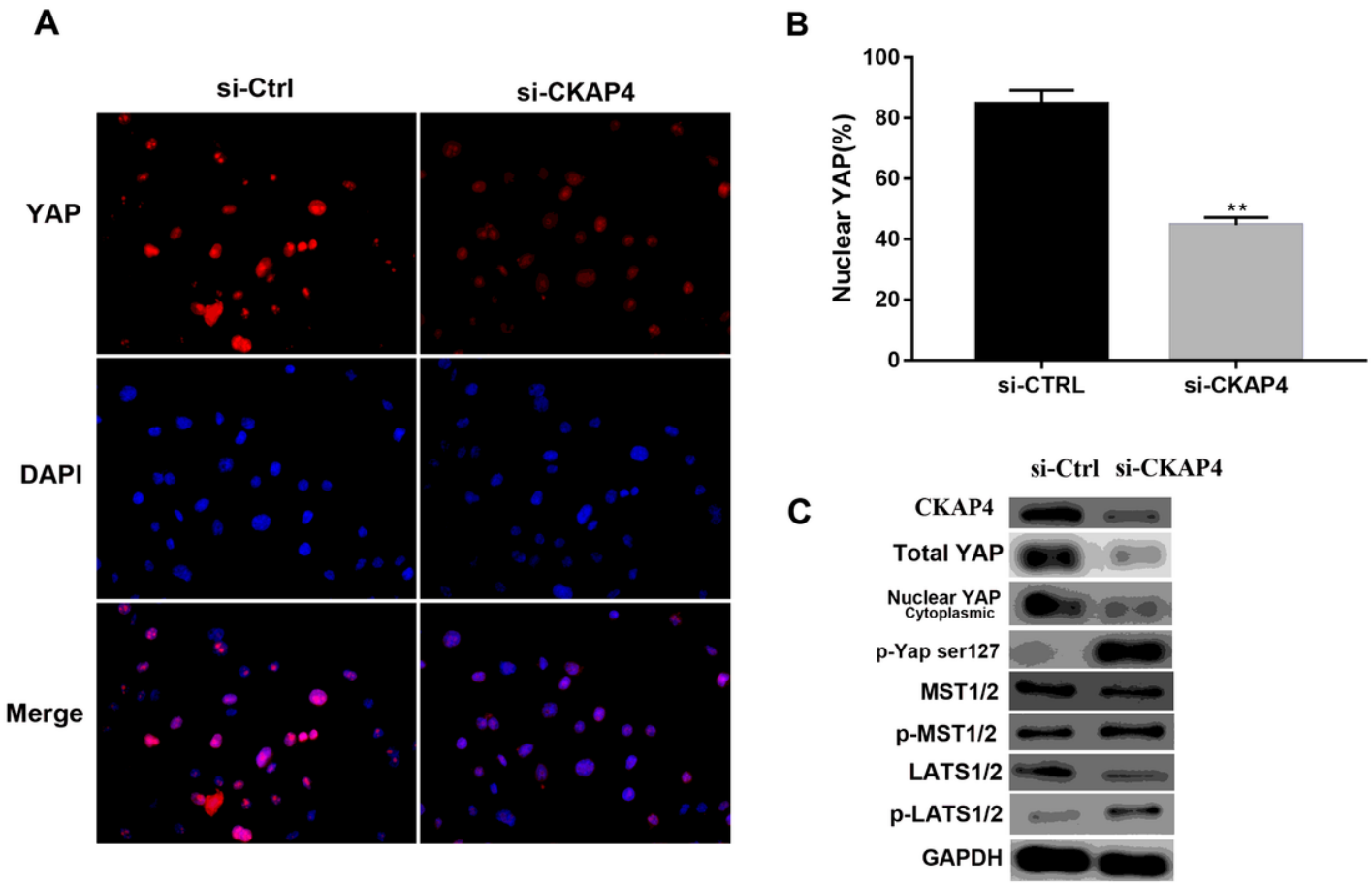

Figure 4

CKAP4 is associated with nuclear translocation of YAP. VSMCs were treated with negative control siRNA, or CKAP4 siRNA (siCKAP4) for 24 h, respectively. (A) Immunofluorescence staining showed nuclear localization of YAP (red) and nuclei (blue) (4, 6-diamidino-2-phenylindole (DAPI)) in VSMCs, cells were treated with negative control siRNA, or CKAP4 siRNA for 24 h, respectively, Scale bar = 20 μm. (B)

Percentage of cells with predominantly nuclear YAP. mean ± SD; n = 10 randomly chosen view-fields. *P < 0.05; **P < 0.01. (C) Western blotting for CKAP4, total YAP, nuclear YAP, phosphorylated YAP S127 (p-YAP s127), MST1/2, p-MST1/2, LATS1 and p-LATS1/2 in whole-cell lysates of VSMCs. Cells were transfected with negative control siRNA, or CKAP4 siRNA for 24 h, respectively.

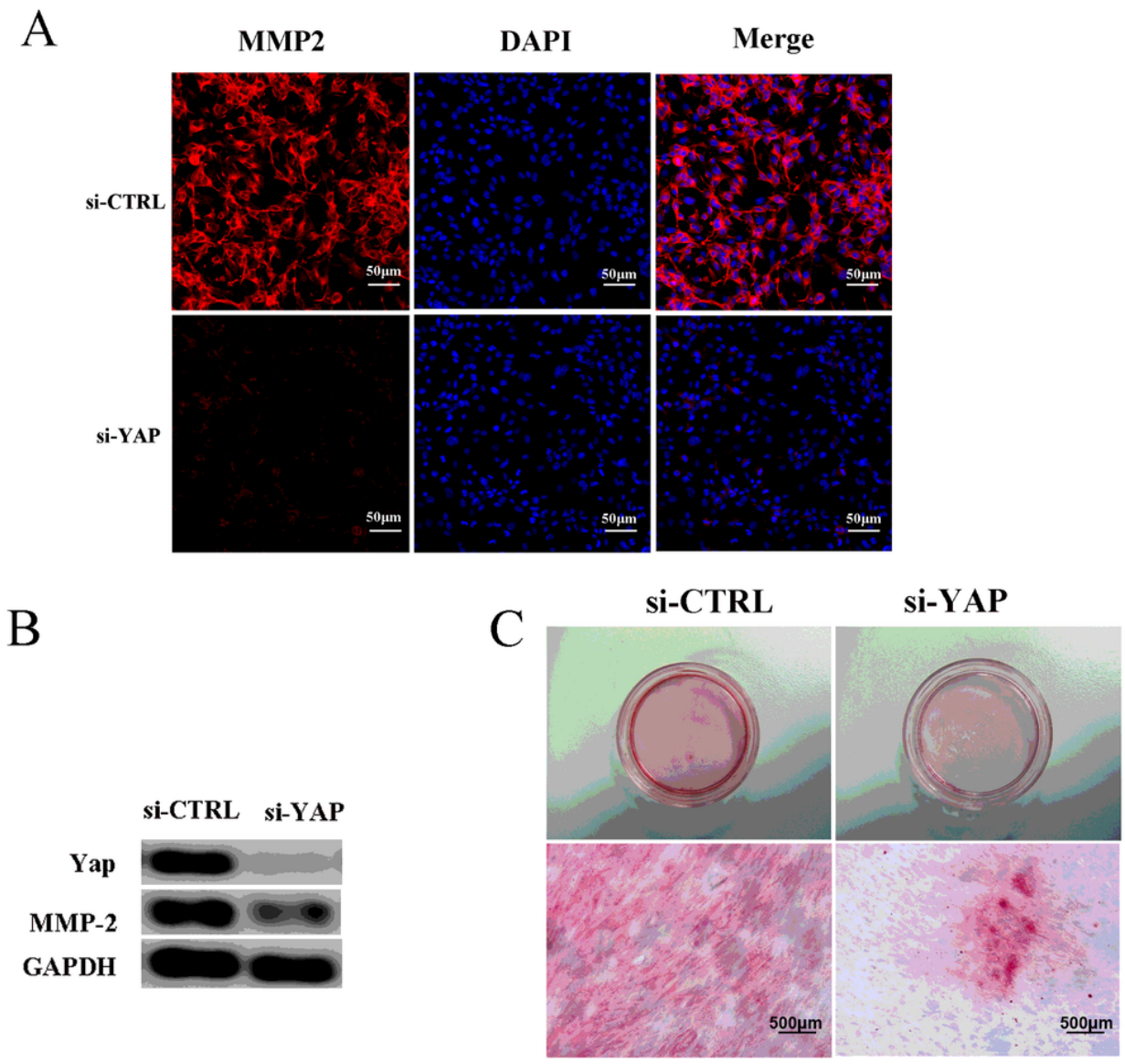

Figure 5

YAP is an upstream regulator of MMP2. VSMCs were treated with negative control siRNA, or YAP siRNA (siYAP) for 24 h, respectively. (A) Immunofluorescence staining of MMP-2 (red) and DAPI (blue) in VSMCs, cells were treated with negative control siRNA, or YAP siRNA for 24 h, respectively. Scar bars, 20 μm. (B) Western blotting analysis of YAP and MMP2 of cells treated with siYAP. (C) Alizarin red staining

was performed on VSMCs incubated under different conditions for 14 days with media replacement every 3 days.

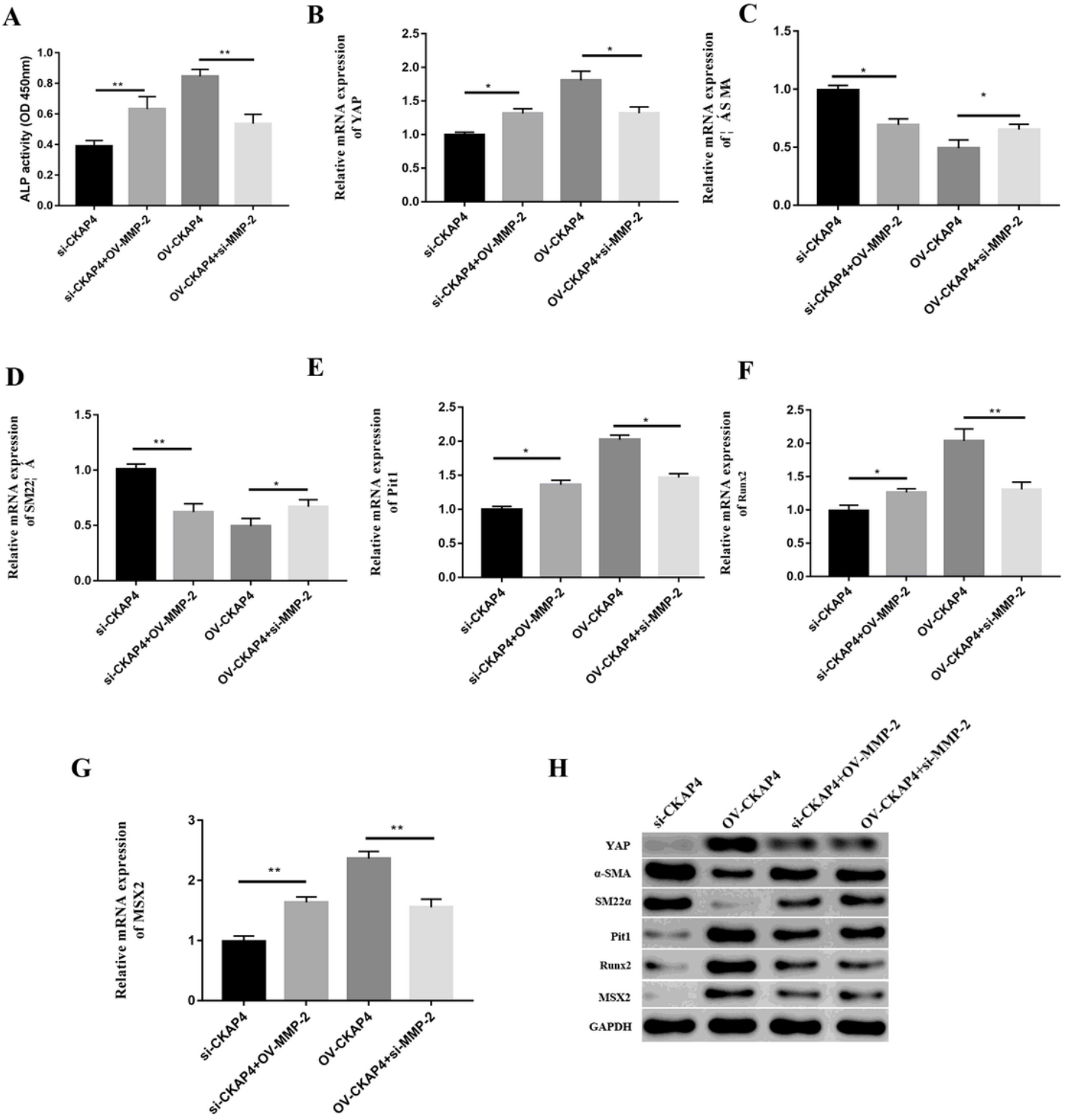

Figure 6

CKAP4 promotes VSMCs calcification via YAP/MMP-2 pathway. (A) ALP activity was expressed as the mean ± SD of at least three simultaneous replicates. (B-H) Expression of YAP, different smooth cell and osteogenesis marker were determined by qRT-PCR and western blotting in VSMCs exposed to

differentiation medium for 24 h. *P < 0.05, **P < 0.01. Abbreviations: si-CKAP4, silencing of CKAP4; si-CKAP4+OV-MMP2, silencing of CKAP4 and overexpression of MMP2; OV-CKAP4, overexpression of CKAP4; OV-CKAP4+ si-MMP2, overexpression of CKAP4 and silencing of MMP2.

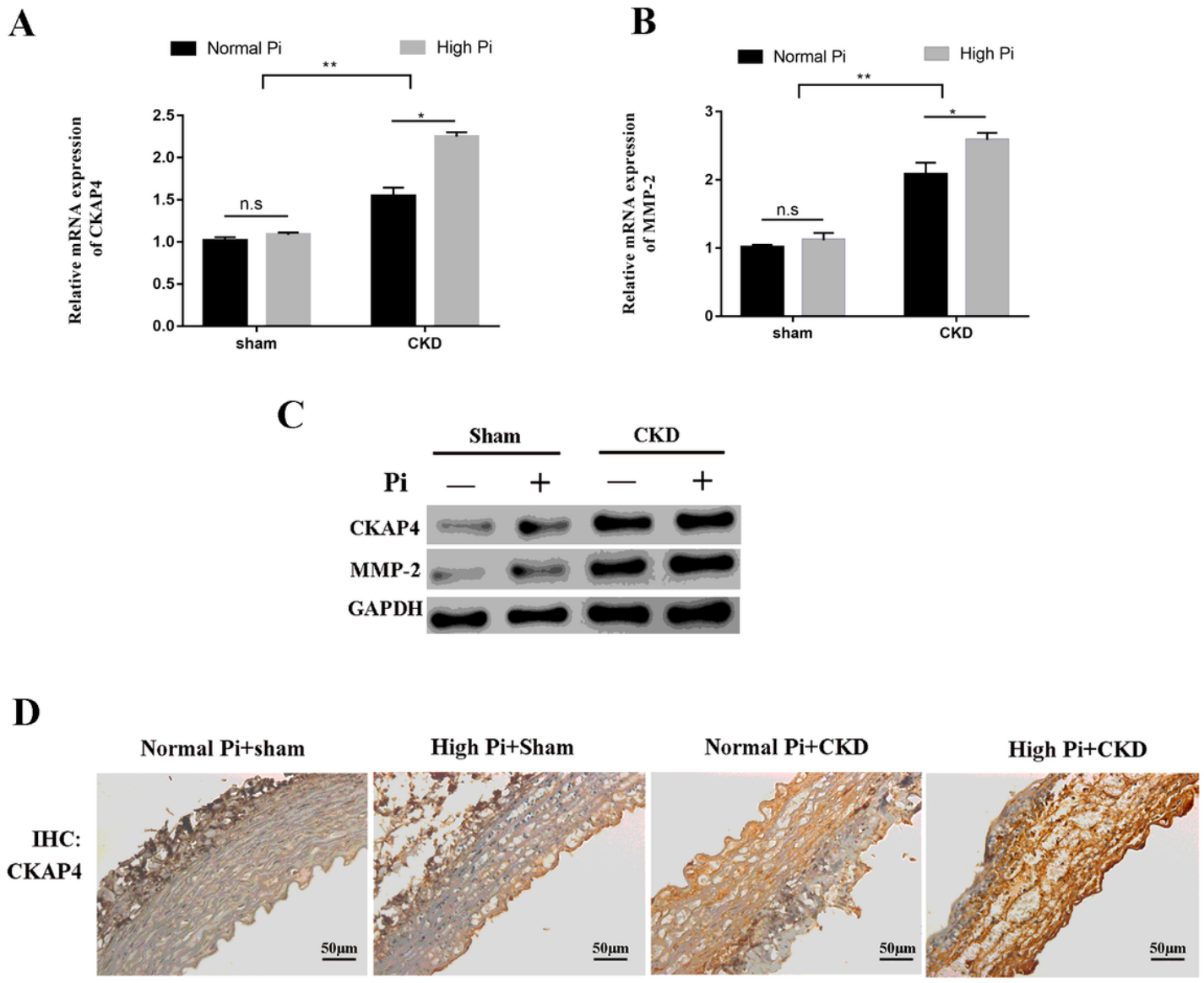

Figure 7

High Phosphate promotes CKAP4 expression in vivo. (A-C) Expression of CKAP4 and MMP2 were detected by qRT-PCR and western blotting. (D) Immunohistochemical staining of CKAP4 protein levels, scale bar = 50μm. *P < 0.05, **P < 0.01.

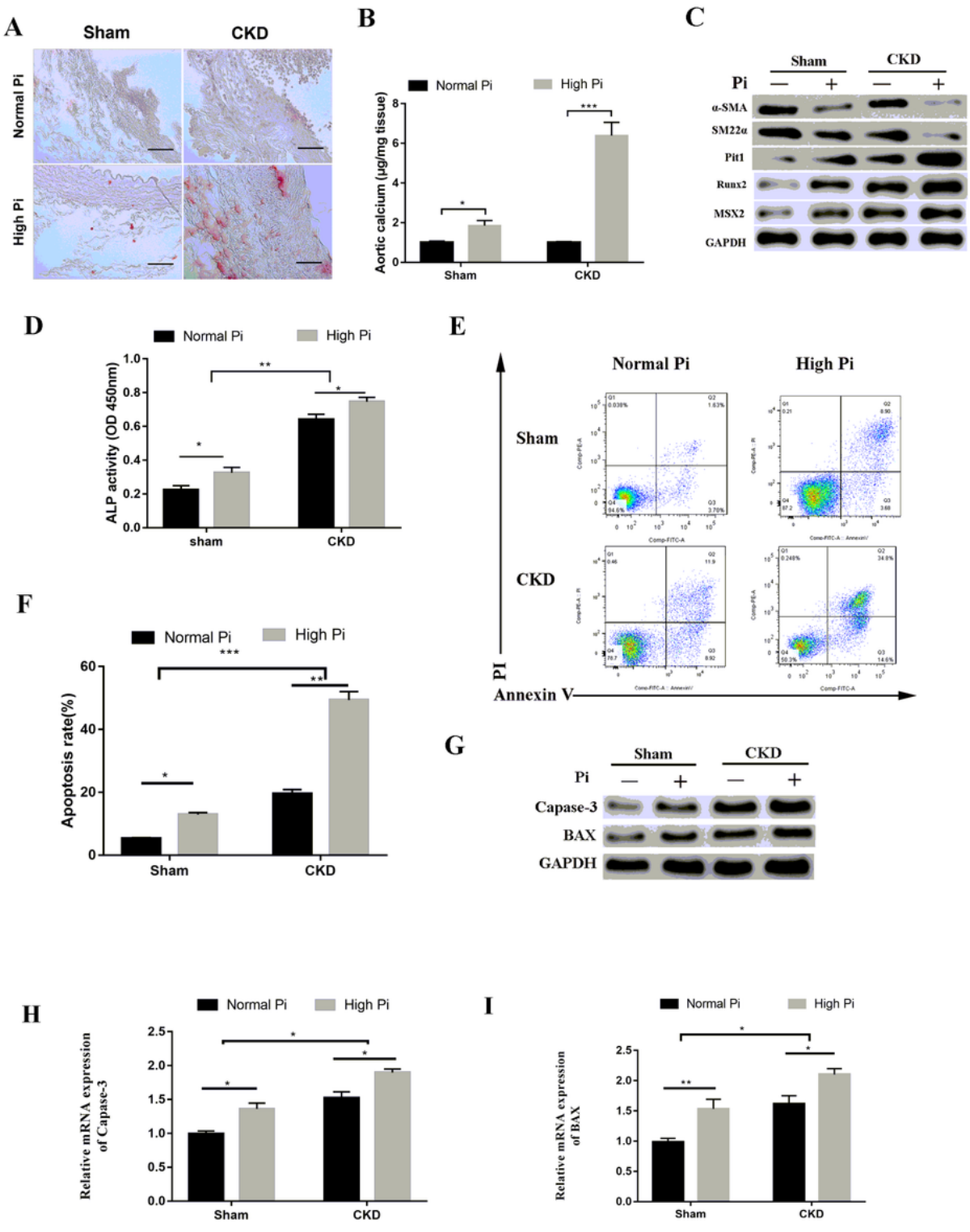

Figure 8

High Phosphate induces aortic calcification in a high CKD model. (A) Representative images of Alizarin Red stained sections of aorta. Scale bar = 50 μm. (B) Calcium content in the thoracic aorta. n = 6 per group. Data are presented as the mean ± SD. *P < 0.05, *** P < 0.001. (C) Expression of different smooth cell and osteogenesis marker were detected by western blotting. (D) ALP activity was expressed as the mean ± SD of at least three simultaneous replicates. (E-F) Analysis of apoptosis rates by flow cytometry

and quantification. Data are expressed as the mean ± SD (n = 3). (G-I) Expression of Capase-3 and Bax detected by qRT-PCR and western blotting. *P < 0.05, **P < 0.01, ***P < 0.001.

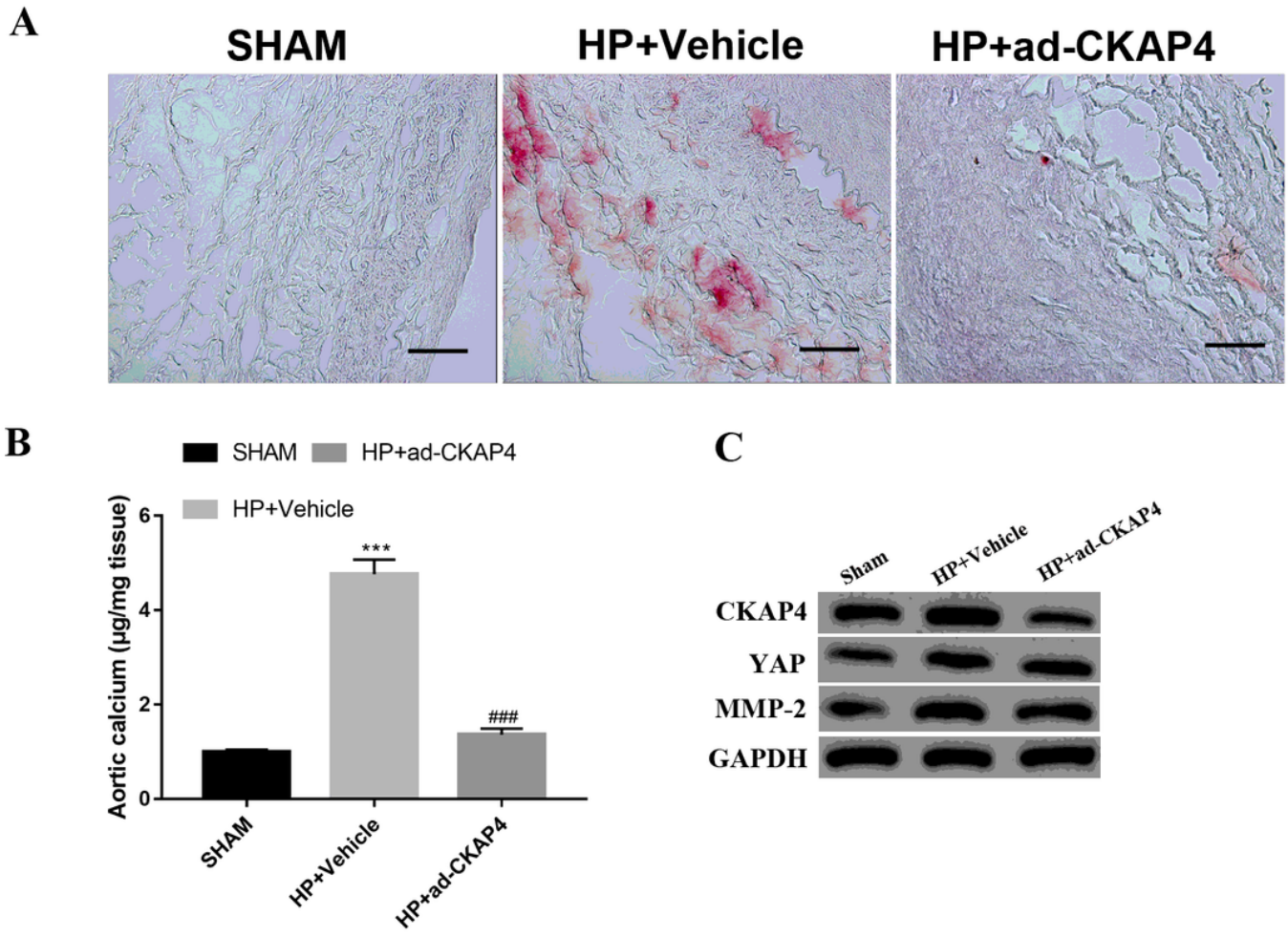

Figure 9

CKAP4 inhibition attenuates vascular calcification in CKD mice. CKD mice were administered with scramble or siCKAP4 lentivirus via tail vein injection and placed on high phosphate diet for 12 weeks. (A) Representative images of alizarin red stained sections of aorta. Scale bar = 50 μm. (B) Calcium content in the tissues of thoracic aorta. n = 6 per group. Data are presented as the mean ± SD. *P < 0.05, ***P < 0.001 vs. Sham###P < 0.001 vs. HP+Vehicle. (C) Expression of CKAP4, YAP, MMP2 were detected by WB. Abbreviations: HP+Vehicle, high phosphate diet + vehicle, HP+ad-CKAP4, high phosphate diet + silencing of CKAP4.